We are IntechOpen, the world's leading publisher of Open Access books Built by scientists, for scientists

6,900
Open access books available

185,000
International authors and editors

200M
Downloads

Our authors are among the

154
Countries delivered to

TOP 1%
most cited scientists

12.2%
Contributors from top 500 universities



WEB OF SCIENCE™

Selection of our books indexed in the Book Citation Index in Web of Science™ Core Collection (BKCI)

Interested in publishing with us?
Contact book.department@intechopen.com

Numbers displayed above are based on latest data collected.
For more information visit www.intechopen.com



Chapter

Triboluminescence: Materials, Properties, and Applications

Zhaofeng Wang and Fu Wang

Abstract

Triboluminescence is one of the types of luminescence that could be activated by mechanical stress. Considering the rising research efforts and achievements in recent years, this chapter provides an overview on the study of triboluminescence. The first part gives a background description regarding the history, research status, and advantages of triboluminescence. Then, we summarize the material systems for triboluminescence in both organics and inorganics. In the third part, we review the properties of triboluminescence, particularly on the unique characteristics and their improvements. Finally, we give a comprehensive summary on the developments of triboluminescent devices for applications in various fields in terms of mechanical engineering, energy, biological monitoring, and sensors as well as lighting, imaging, and displaying.

Keywords: triboluminescence, crystals, spectral characteristics, cycling stability, advanced applications

1. Introduction

Triboluminescence (TL) refers to the phenomenon that materials could emit light when they are mechanically stimulated, such as rubbing, grinding, impact, stretching, and compression [1–3]. TL was first recorded by Francis Bacon in 1605 when breaking the sugar crystals [4]. After that, TL has been found in many solids, such as rocks, quartz, alkaline halide, molecular crystals, and some organic materials [5]. It is estimated that nearly 50% of inorganic compounds and 30% of organic molecular solids have been confirmed to have TL [6]. Because TL could be directly activated by the widely existed mechanical activities in daily life without requiring artificial optical/electrical sources, TL shows great advantages in energy saving and environmental protection [7].

In general, TL could be classified into three types, i.e., fracture TL, plastic TL, and elastic TL [8], as illustrated in **Figure 1**. Among them, the elastic TL has gained the most attention because of its structure nondestructive characteristic which is crucial for practical applications. The present researches of TL are mainly focused on the development of novel TL materials and the performance improvement in terms of brightness, color manipulation, and cyclic stability [9–11]. Based on the efforts in the above aspects, a variety of decent applications of TL materials have been achieved in recent years, covering the fields of mechanical engineering, energy, biological monitoring, and sensors as well as lighting, imaging, and displaying.

In this chapter, we provide an overview of TL, regarding the materials, properties, and applications. Since TL covers a large range from organics to inorganics with emitting types from fracture TL to plastic TL and elastic TL, most of the

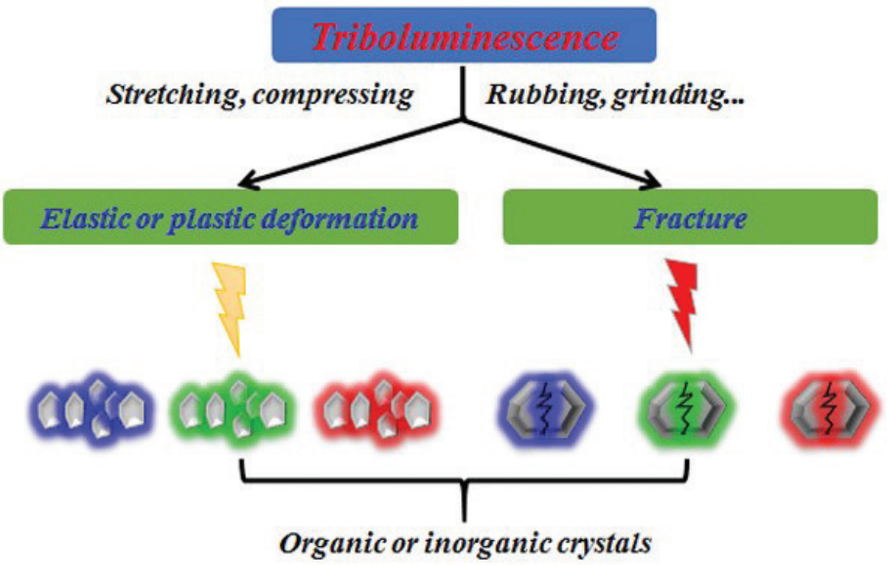


Figure 1.
Illustration of the fracture, plastic, and elastic deformation-induced TL in organic and inorganic crystals.

content of the chapter was focused on the elastic TL of inorganic solids in which the most significant progresses have been made during recent years. We hope that this chapter could provide a deep understanding of TL and stimulated new ideas for further researches.

2. TL materials

2.1 Organic crystals and organometallic compounds

Organic crystals and organometallic compounds represent an important part of TL materials. About 19% of organics and 37% of aromatic compounds are estimated to have TL [12]. According to molecular structure, the TL organic crystals could be divided into nonaromatic organic crystals and aromatic compounds. The main nonaromatic organics include sugar (e.g., D-glucose, lactose, maltose, L-rhamnose, sucrose), tartaric acid/tartrate (e.g., ammonium tartrate, sodium tartrate) and other nonaromatic organics (e.g., L-ascorbic acid, cholesteryl salicylate, cholestenol, ammonium oxalate, disodium hydrogen citrate, aniline hydrochloride) [13–15]. The main aromatic compounds are coumarin, acenaphthene, phthalic anhydride, phenanthrene, phenol derivatives, 9-anthryl carbinol, N-phenyl-substituted imides, carbazole derivatives, hexaphenylcarbodiphosphorane $(Ph_3P)_2C$, and some aggregation-induced emission compounds (e.g., tetraphenylethene compounds, N-substituted phenothiazine, aryl dioxaborolane, N-substituted dihydroacridine) [16–18]. The above aromatic compounds always possess distinctive TL characteristics because of their peculiar molecular structure, and their TL should arise from the spin-allowed/spin-forbidden electron transition of molecular excited state (π-π^* transition), likewise with their photoluminescence (PL). Moreover, impurities play special roles in TL of some compounds.

Organometallic compounds, including rare earth and transition metal complexes, have also featured TL. The typical examples are some β-diketone complexes of Ln^{III} ion (Ln = Eu, Sm, Pr, Yb, Tb, Gd, or Nb). Among them, the europium complexes (EuD_4TEA and its doped forms) generate extremely bright and daylight-visible red-orange TL, which is much stronger than that of the others [19]. But these

complexes show a very sharp emission band corresponding to the f-f transition of Eu^{3+} ions. The transition metal-based complexes are mainly Mn^{II}, copper^{I}, and Pt^{II} complexes, such as $Mn(Ph_3PO)_2X_2$ (X = Cl, Br), $(MePh_3P)_2MnCl_4$, $Cu(NCS)(py)_2(PPh_3)$, and Pt(ipyim)(bipz), which give a broad emission band [20].

2.2 Inorganic compounds

The inorganic TL compounds are composed by hosts and doping luminescent centers. The inorganic hosts include the halides (e.g., KCl, KBr, NaF, RbBr, and RbI [21]), oxides (e.g., Al_2O_3 [22] and ZrO_2 [23]), sulfides (e.g., ZnS [24]), oxysulfides (e.g., CaZnOS [10] and BaZnOS [25]), aluminates (e.g., $SrAl_2O_4$ [1], $Sr_3Al_2O_6$ [7], and $CaYAl_3O_7$ [9]), silicates (e.g., $Sr_2MgSi_2O_7$ and $SrCaMgSi_2O_7$ [26]), phosphates (e.g., Li_3PO_4 [27] and $SrMg_2(PO_4)_2$ [28]), borates (e.g., BaB_4O_7 [29]), titanates (e.g., $BaTiO_3$ and $CaTiO_3$ [30]), niobates (e.g., $Ca_2Nb_2O_7$ [31] and $LiNbO_3$ [32]), stannates (e.g., Sr_2SnO_4 [33]), sulfates (e.g., $BaSO_4$ [34]), and oxynitrides (e.g., $BaSi_2O_2N_2$ [35]). Rare earth ions are the common doped ions in inorganic TL compounds, such as Eu^{2+}, Eu^{3+}, Pr^{3+}, Dy^{3+}, Ce^{3+}, Tb^{3+}, Er^{3+}, and Sm^{3+} [4]. The other metal ions, like Mn^{2+}, Cu^{+}, and Ti^{4+} ions [23, 36], are also employed as the luminescent centers in inorganic TL compounds. To date, the well-recognized inorganic compounds with bright TL are $SrAl_2O_4$:Eu^{2+}, Dy^{3+} (SAOED), and ZnS:Mn^{2+}/Cu^{+}.

3. TL properties

3.1 Spectral characteristics

In many organic and inorganic systems, the TL spectra are consistent with the PL spectra, suggesting they possess the same emitting processes. The differences between TL and PL lie in the excitation/activation processes that TL originates from the release of the trapped carries or the piezoelectric effect under mechanical stimuli. In some systems, like BaZnOS:Mn^{2+} [25], the compression-induced TL and rubbing-induced TL exhibit 24 nm and 48 nm blueshift, respectively, compared to that of PL (**Figure 2**). Such phenomenon could be ascribed to the conduction band and valence band tailoring by piezoelectric fields.

In piezoelectric materials, there is also obvious difference on the concentration quenching between PL and TL. For example, the quenching concentrations of Pr^{3+} in $CaNb_2O_6$, $Ca_2Nb_2O_7$, and $Ca_3Nb_2O_8$ for TL are 0.25 mol%, 0.1 mol%, and 0.075 mol%, respectively, while the values for PL are 0.5 mol%, 0.3 mol%, and 0.1 mol%, respectively [31]. The decreased quenching concentration of TL was attributed to the participation of piezoelectric field in delivering the energy from traps to quenching centers.

3.2 Cycling stability

The TL of organic molecules or complexes mostly originates from the fracture of crystals, and thus there is no cycling stability for such materials. For the TL along with the nondestructive structure, mainly referring to the piezoelectric effect and de-trapping-induced TL, the cycling stability is particularly important. The TL aroused by piezoelectric effects usually exhibits stable luminescence when activated by cyclic mechanical tests [37]. For example, the Pr^{3+}-doped $LiNbO_3$ could keep its TL intensity for more than 100 cycles [32]. ZnS:Cu/PDMS composites could maintain the TL intensity up to 30,000 cycles of stretching, and the intensity still reached 65% of the initial one without a color change even after 100,000 cycles of

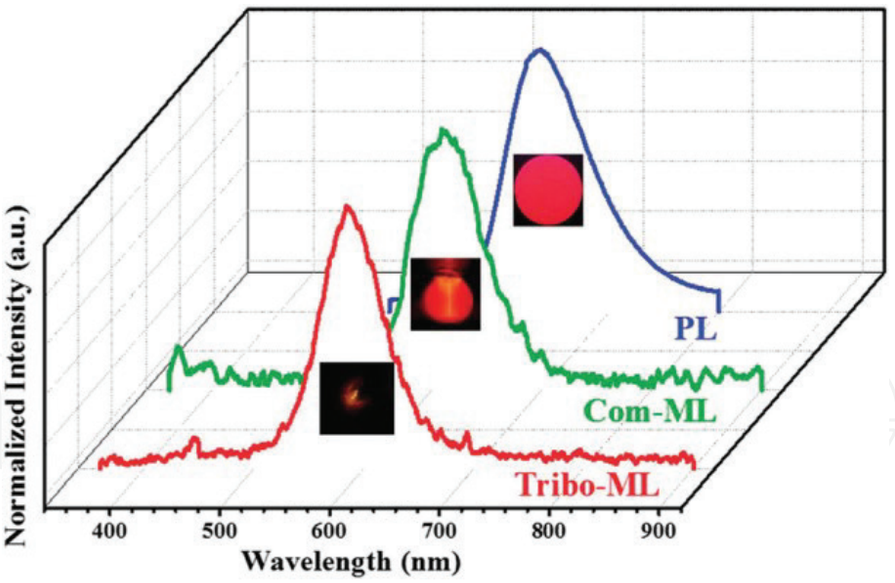


Figure 2.
Spectral comparison of the PL, compression-induced TL, and rubbing-induced TL in BaZnOS:Mn2+. Reproduced by permission of the Royal Society of Chemistry [25].

tests [38]. However, for the TL aroused by the de-trapping of carriers in structure, intensity degradation would be serious during cycling tests, i.e., such materials showed poor cycling stability [39, 40]. To overcome the above issue, great efforts have been made based on the TL mechanism in terms of the de-trapping processes. Researchers proposed a strategy to improve the cycling stability of the de-trapping-induced TL by applying an extra UV irradiation source to ensure the balance between the trapping and de-trapping of carries [11]. The power density played a key role to stabilize the TL intensity, and the effective power density was determined to be 1000 mW/cm^2 as shown in **Figure 3** [41].

3.3 Intrinsic structure-dependent TL

The TL characteristics could be directly modulated by varying the concentration of luminescent centers. Generally, there is a concentration quenching phenomenon in terms of TL intensity. In CaZnOS:Mn^{2+}, the increase of the doping concentration of Mn^{2+} could not only vary the TL intensity with a trend that increases first and then decreases but also arouse a redshift on the TL spectra with the emitting color manipulated from orange to red [10]. In addition, the chemical composition of the hosts, namely, the variation of the defect phases or traps, could also cause significant variations on the TL intensity and color. In (Ba,Ca)TiO_3:Pr^{3+}, the co-dopant of trivalent rare earth ions, such as La^{3+}, Y^{3+}, Nd^{3+}, Gd^{3+}, Yb^{3+}, and Lu^{3+}, could greatly improve the TL intensity, in which Gd^{3+} could enhance the intensity more than 61% [30]. This is because that the co-dopant of the above ions could increase the concentration of the carries in traps and thus lead to more luminescence emitted under mechanical stimuli. In $Sr_2MgSi_2O_7$:Eu^{2+}, when part of Sr^{2+} was substituted by Ca^{2+} or Ba^{2+}, the TL intensity and emitting color could be adjusted simultaneously [26]. $SrBaMgSi_2O_7$:Eu^{2+} showed the lowest TL intensity compared to that of $Sr_2MgSi_2O_7$:Eu^{2+} and $SrCaMgSi_2O_7$:Eu^{2+}. The replacement of Sr^{2+} by Ca^{2+} or Ba^{2+} in $Sr_2MgSi_2O_7$:Eu^{2+} could further manipulate the emission band in a wide range from 440 nm to 499 nm. Researches also showed that the TL performance is dependent on the crystal size. In sucrose crystals, the TL intensity significantly increased with increasing crystal size (**Figure 4**), which could be explained by piezoelectric mechanism [42].

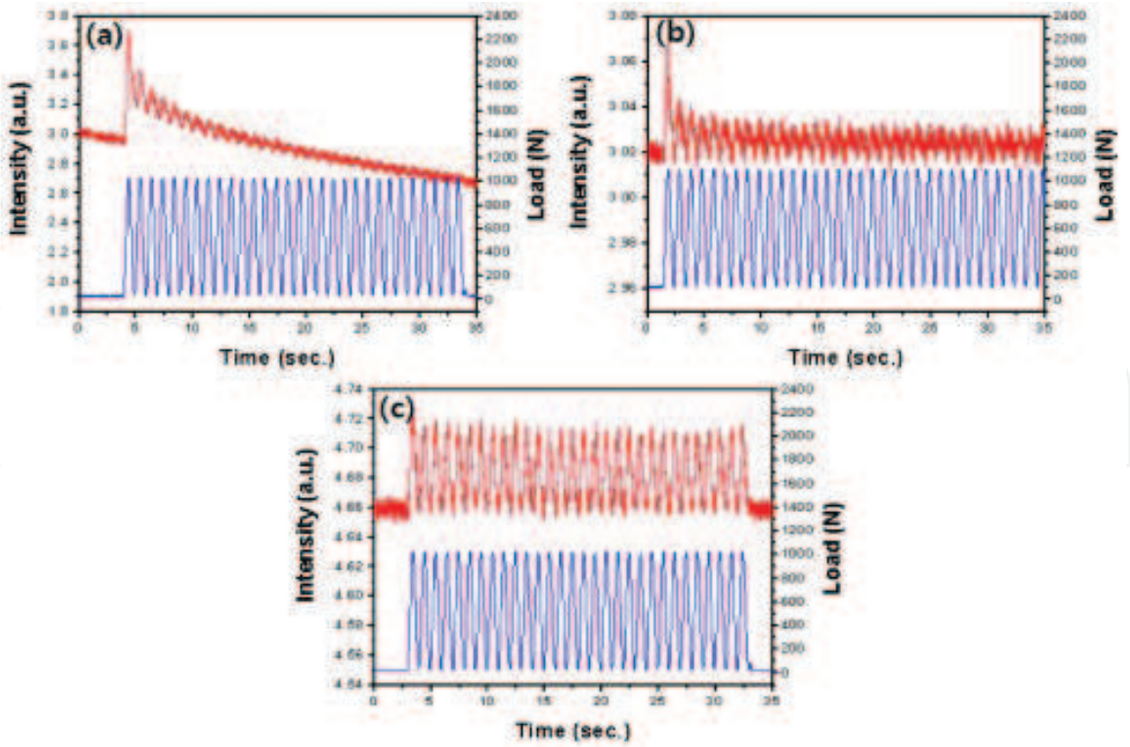


Figure 3.
TL intensity of SAOED response to the cyclic load at a frequency of 1 Hz under different irradiation conditions: (a) with UV irradiation turned off; (b) under a UV irradiation with a power density of 200 mW/cm2; (c) under a UV irradiation with a power density of 1000 mW/cm2. Reproduced by permission of the OSA Publishing [41].

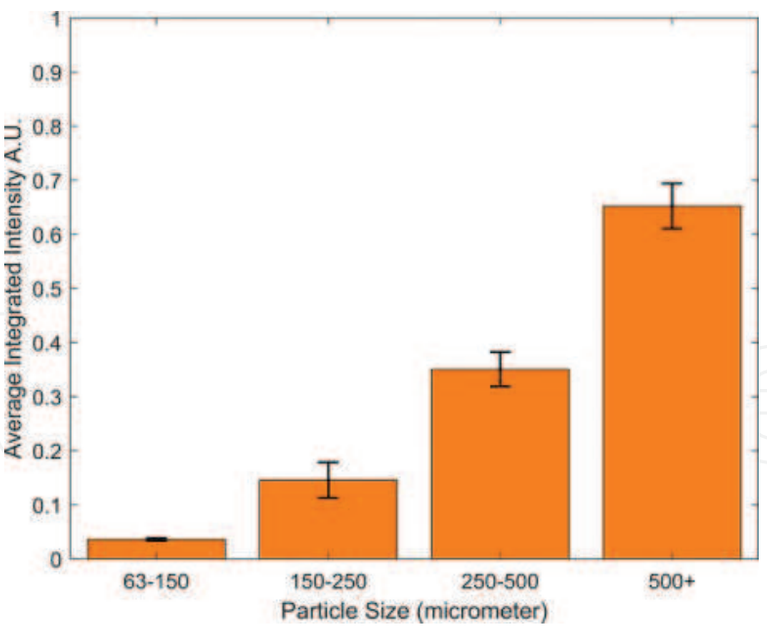


Figure 4.
TL integrated intensity on dependent of particle sizes of sucrose crystals. Reproduced by permission of the American Chemical Society [42].

3.4 External factor-dependent TL

The TL powders could be directly stimulated by ultrasonication or impact. The ultrasonic TL is dependent on the ultrasonic power with a linear relationship [43]. The impact-induced TL is strongly affected by the impact velocity or impact energy [2, 44]. When TL powders were composited in various matrices, other mechanical

actions, such as rubbing, stretching, and compression, would be employed for TL. The intensity of the rubbing-induced TL shows relationships to both the applied normal load and the friction velocity [43]. For the stretching-induced TL, the elastic modulus plays a key role on the critical strain [45]. In addition, TL intensity varies along with the change of strain levels and stretching speeds [7]. For the compression-induced TL, it depends on the applied load as well as the deformation rate [31, 37].

4. Applications

TL materials could be composited in a variety of hosts, such as polymer matrices and metal bulk materials. The as-fabricated TL composites could emit light under the stimulus of mechanical behaviors for various applications. Because $SrAl_2O_4:Eu^{2+}$ and $ZnS:Mn^{2+}/Cu^{+}$ are the well-recognized intense TL materials, the present applications almost focus on them.

4.1 Structural health monitoring

The TL composites could be directly stimulated by the inner stress, showing application perspectives in structural health monitoring of devices, machines, and buildings [46–48]. To date, TL materials have been well employed to visualize and monitor the stress distribution as well as the fatigue crack initiation and propagation of matrices [1, 49, 50]. The sensitization of stress distribution in solids was first conducted by C-N. Xu et al. [1] They composited the green-emitting $SrAl_2O_4:Eu^{2+}$ TL powders in epoxy resins and confirmed that the TL behaviors of the $SrAl_2O_4:Eu^{2+}$/epoxy composites under a compressive load of 1000 N could reflect the stress distribution based on the experimental and simulative results. The $SrAl_2O_4:Eu^{2+}$/epoxy composites were further employed to realize the measurements of instantaneous R-curves and bridging stress in a fast-propagating crack system (**Figure 5**) [51].

Based on the above pioneering achievements, researchers successfully developed the structural health monitoring applications of TL materials in steel box girders [52], hydrogen storage cylinders [53], and gas pipelines [54]. Compared with the conventional monitoring methods by electrical and magnetic signals, the approach by TL signals shows advantages of contactless, wireless, convenient, and visualization [49, 52].

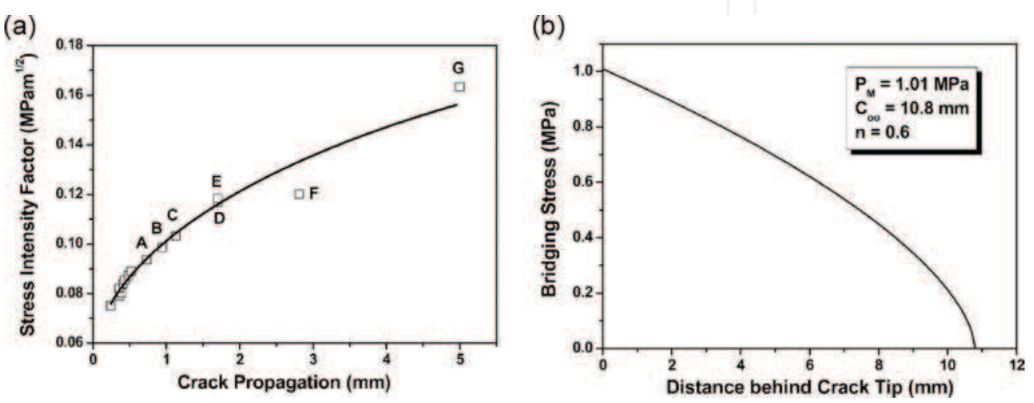


Figure 5.
Experimental R-curve and bridging stress distribution in the crack wake based on the TL of SAOED. Reproduced by permission of Elsevier B.V. [51].

4.2 Impact/load sensor

When TL materials undergo loading or impact, the emitted luminescence shows one-to-one correspondence between the emission intensity and impact/loading energy, which could be utilized to develop impact/load sensors to record the related mechanical information [2]. However, for the sensors fabricated from $SrAl_2O_4:Eu^{2+}$, the prominent problem is that the TL intensity will be decreased along with the increase of impact times or loading time, i.e., $SrAl_2O_4:Eu^{2+}$ shows poor cycling stability that goes against for its applications as impact/load sensors [41, 44]. Researchers further found that when an ultraviolet (UV) irradiation source with a certain power density was applied, $SrAl_2O_4:Eu^{2+}$ could keep the TL intensity stably based on the balance of trapping and de-trapping of the carriers in structure [41, 44]. The proposed $SrAl_2O_4:Eu^{2+}$-based sensor under UV irradiation could stably sensitize the applied load both in dynamic and static states (**Figure 6**) [41]. Differing from $SrAl_2O_4:Eu^{2+}$, ZnS:Mn/Cu showed almost no TL intensity degradation along with the increase of cycle numbers because of the piezoelectric effect, which could be directly used for impact/load sensor applications without needing an extra UV irradiation [37, 55].

4.3 Lighting, imaging, and displaying

The exploited devices for lighting, imaging, and displaying are mainly fabricated from ZnS:Mn/Cu and elastomer matrices. The as-fabricated ZnS:Cu/PDMS flexible composites showed bright and durable TL under stretching with a brightness of ca. 120 cd/m^2 and durability over 10,000 cycles [38]. The composites could be further fabricated into fabrics with patterns that could be applied for imaging and displaying as presented in **Figure 7** [56].

In addition to the stimulus of stretching and rubbing, the TL composites could also be activated by various mechanical sources, such as wind [5], magnetic field [57], and ultrasonic wave [58], which fulfill the requirements of green and sustainable developments. For practical applications in lighting and displaying, the TL flexible devices with a white light or multicolored emissions are required, and a variety of strategies have been proposed. For example, Jeong et al. employed ZnS:Cu, Mn and ZnS:Cu as the orange and green TL materials, respectively, and fabricated ZnS-based flexible composites, in which TL color manipulation including a warm white light was demonstrated by adjusting the component ratios of

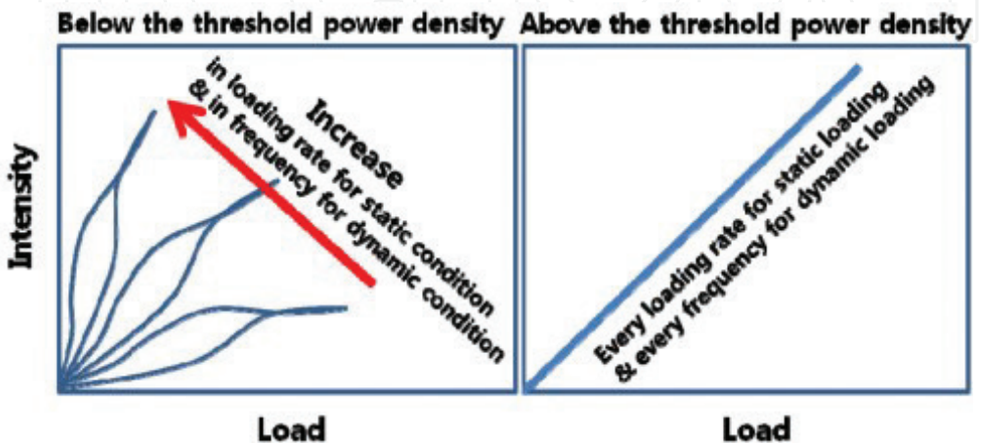


Figure 6.
Load responsiveness of SAOED in static and dynamic states with UV irradiation turned on and turned off. Reproduced by permission of the OSA Publishing [41].

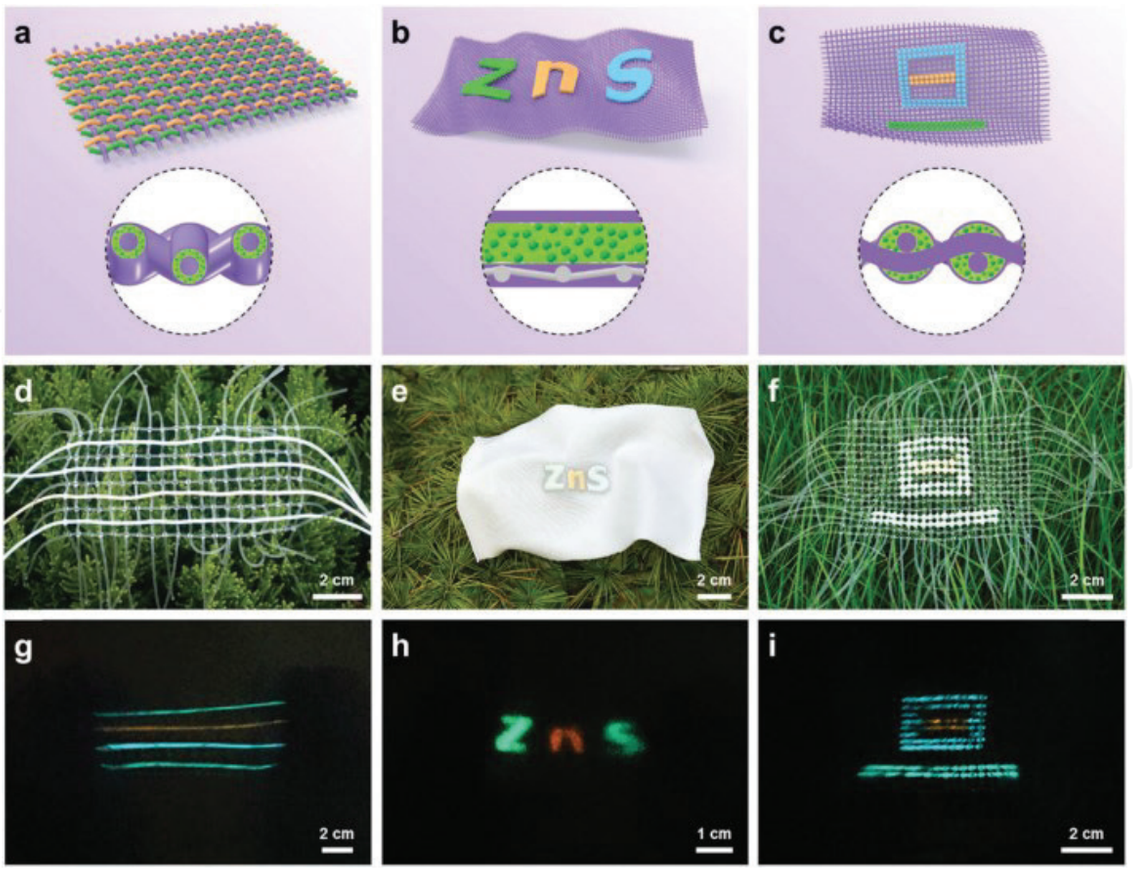


Figure 7.
TL fabrics based on the doped ZnS (a) fibers, (b) ribbons, and (c) dots; corresponding (d–f) optical and (g–i) TL photographs of the fabrics in (a–c). Reproduced by permission of the Royal Society of Chemistry [56].

ZnS:Cu, Mn and ZnS:Cu [36]. They further presented a strategy for the TL color manipulation of doped ZnS by physically combining fluorescent dyes in PDMS elastomers based on the energy transfer between the TL of doped ZnS and the PL of dyes [59]. Hao and his co-workers also realized the remote tuning of TL color of ZnS:Al, Cu/PDMS composites by modulating the frequency of magnetic field [60]. In addition, flexible devices with dual-mode emissions, i.e., EL and TL, have also been developed for imaging and displaying [59, 61].

4.4 Pressure sensor

The TL flexible composites exhibit luminescent signals dependent on the applied pressure. Based on such performance, Wang et al. developed a ZnS:Mn-based pressure sensor for both single-point dynamic pressure recording and 2D planar pressure mapping with a high spatial resolution of 100 μm and a fast response time less than 10 ms [24]. The pressure sensor was further used as a flexible handwriting device that could collect the information of both signatures and signing habits as shown in **Figure 8**, exhibiting high-level security compared with the existing technologies. They further introduced the single-electrode triboelectric nanogenerator in the ZnS:Mn-based flexible composites and obtained a full dynamic-range pressure sensor for the visualization of pressure distribution both in low pressure regimes (< 100 kPa) and high-pressure regimes (> 1 MPa) with an excellent pressure sensitivity of 6 MPa^{-1} [62]. In addition, $CaZnOS:Er^{3+}$ thin-film was prepared, which possessed the pressure and temperature sensing based on its TL and upconversion luminescence [63].

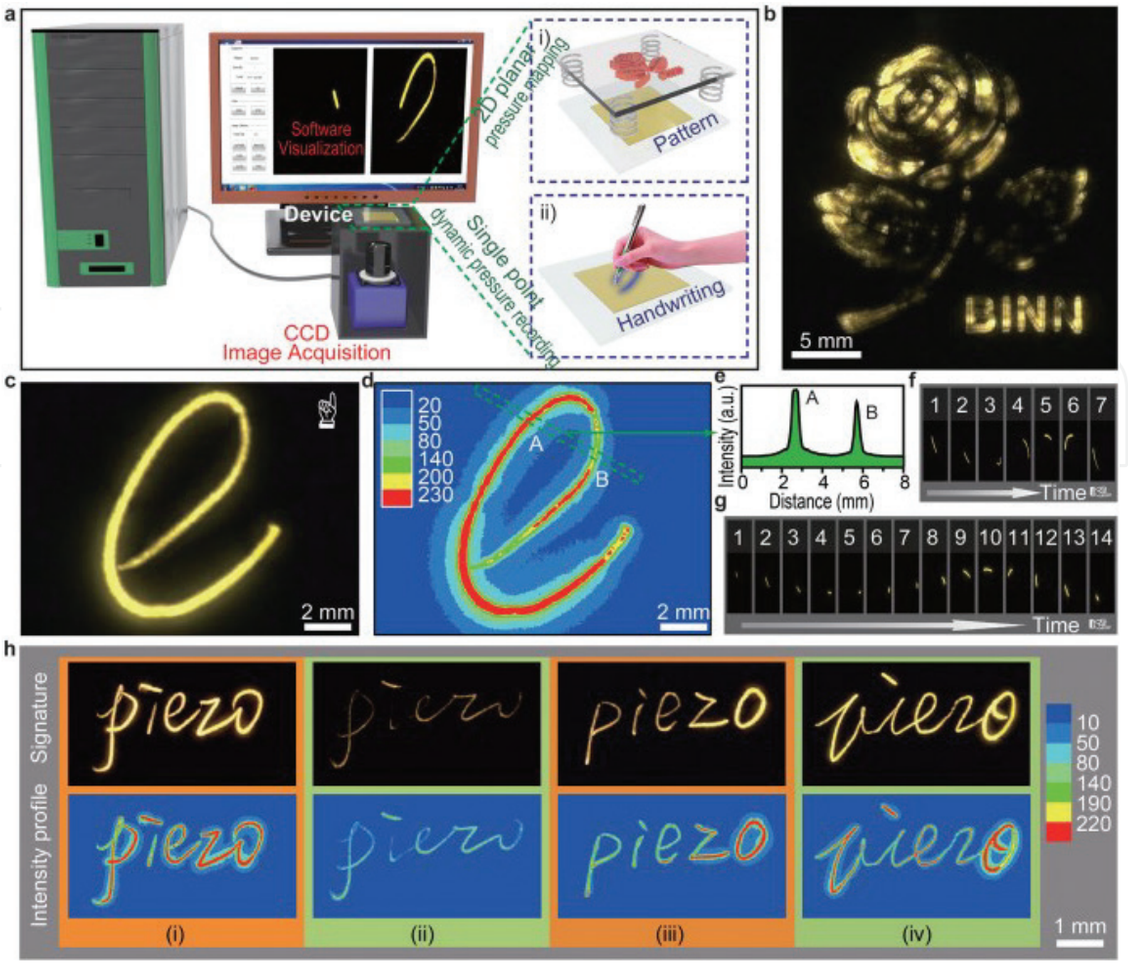


Figure 8.
Flexible handwriting device based on the TL of ZnS:Mn for visualization of dynamic pressure distributions: (a) schematic illustration of the system; (b) visualization of 2D planar pressure distribution; (c-h) visualization of the signing process. Reproduced by permission of Wiley-VCH [24].

4.5 Stress/strain sensor

When the TL materials are introduced in elastic matrices, stress/strain sensor could be obtained. At present, the widely employed TL materials for fabricating stress/strain sensors are ZnS:Mn, ZnS:Cu, and $SrAl_2O_4$:Eu, because of their prominent TL properties as well as the one-to-one correspondence between the TL intensity and stress/strain. Yun et al. [64] further found that the co-dopant of Dy^{3+} in $SrAl_2O_4$:Eu could improve its performance as stress sensor based on the sensitivity. In addition to sense the stress or strain by analyzing the TL intensity, the risetime and decay time of TL during cyclic elastic deformation of $SrAl_2O_4$:Eu were also demonstrated to be suitable for evaluating the change of the strain energy [65]. Moreover, a calibration method for $SrAl_2O_4$:Eu, Dy-based thin-film sensor was proposed to enable quantitative full-field strain measurements in pixel-level resolution [66]. Qian et al. [45] prepared ZnS:Mn/Cu@Al_2O_3/PDMS flexible composites and adjusted the elastic modulus by introducing SiO_2 nanoparticles. They finally obtained a TL stress/strain sensor that could be driven by weak mechanics of skin movements.

In the very recent work [7], $Sr_3Al_2O_6$:Eu with bright and tunable PL and TL was presented when it was composited in PDMS elastomers. By combining the wavelength selectivity of PL and dynamic stress responsiveness of TL, a multimode stretching/strain sensor was developed by a bilayered structure design of $Sr_3Al_2O_6$:Eu/PDMS composites with coating a light-shielding layer of Au atop

(as shown in **Figure 9**). The fabricated sensor could sense the stretching states and strain levels simultaneously, breaking the limit of static strain sensing in previous researches.

4.6 Mechanics-light-electricity conversion

The TL materials could convert mechanics into light, which could be further utilized to generate electricity for various applications. When the $SrAl_2O_4$:Eu/epoxy TL composites were combined in a commercial silicon solar cell, the mechanics-light-electricity conversion could be achieved [67]. In addition to the generation of electricity by utilizing the mechanics-induced luminescence, TL materials could be combined with a nanogenerator and convert the input mechanical stimuli to electric and light simultaneously [68]. The TL materials could also be composited with a photocatalyst to realize the catalysis activity in dark under the stimuli of mechanics [69]. The above conversion systems based on TL show great perspectives for applications in dark environments, such as deep sea and polar night region.

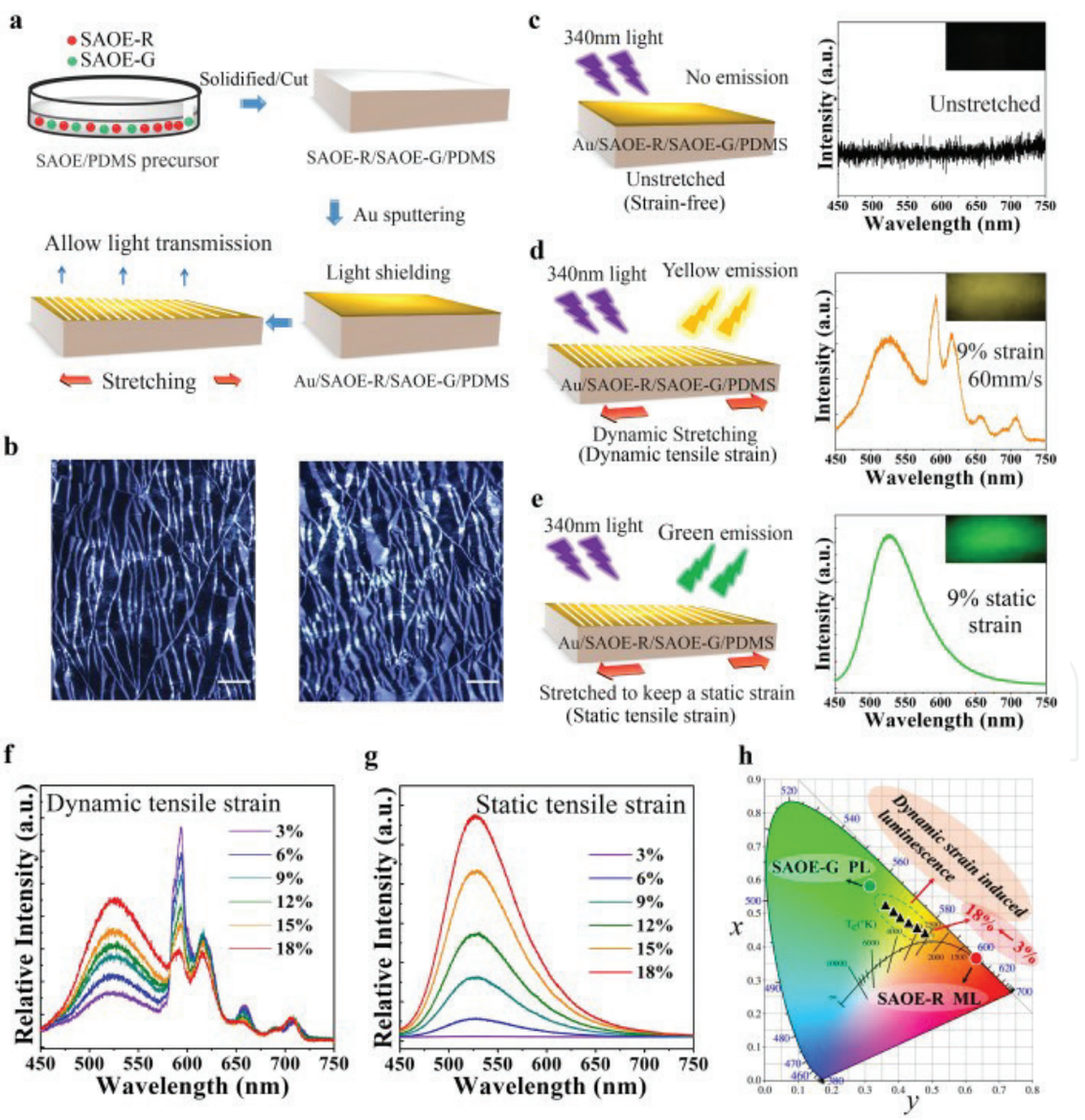


Figure 9.
Multimode stretching/strain sensor based on the TL and PL of Sr3Al2O6:Eu: (a) fabricating process; (b) crack opening when stretched, scale bar: 100 μm; (c–e) stretching state responses; (f–g) strain level responses; (h) corresponding color conversion based on various dynamic strain levels. Reproduced by permission of Wiley-VCH [7].

4.7 Biological applications

Because some of the TL materials show good biocompatibility, such as the rare earth-doped oxide ceramics, they are promising for the detection of mechanical behaviors in biological tissues/organs. The $SrAl_2O_4$:Eu TL powders was applied in the synthetic bone, and the related mechanical dynamic environment was monitored with a high-definition and high-speed visualization [70]. SAOED powders were also applied in artificial tooth for occlusal examination [71]. The composition of SAOED in the commercial denture base resin (DBR) could not only endow with bright TL but also improve its mechanical performance. As a result, an artificial tooth model with SAOED was made in which bright and sensitive TL could be directly observed to guide clinicians to purposefully adjust the occlusal surface until a balanced occlusion established.

5. Conclusions

In summary, we present a comprehensive overview on the study of TL. The material systems in both organics and inorganics, unique spectral characteristics, and TL performance, as well as the representative applications in various fields, are included. We hope that this chapter could help researchers in the field to gain a comprehensive and in-depth understanding of TL and stimulate continued interests and endeavors in this area to promote more innovative applications.

Acknowledgements

The authors thank the support from the Natural Science Foundation of Gansu Province (17JR5RA319) and the CAS Pioneer Hundred Talents Program.

Conflict of interest

The authors declare no conflict of interest.

Author details

Zhaofeng Wang* and Fu Wang
State Key Laboratory of Solid Lubrication, Lanzhou Institute of Chemical Physics, Chinese Academy of Sciences, Lanzhou, Gansu, China

*Address all correspondence to: zhfwang@licp.cas.cn

IntechOpen

© 2018 The Author(s). Licensee IntechOpen. This chapter is distributed under the terms of the Creative Commons Attribution License (http://creativecommons.org/licenses/by/3.0), which permits unrestricted use, distribution, and reproduction in any medium, provided the original work is properly cited. CC BY

References

[1] Xu C-N, Watanabe T, Akiyama M, Zheng X-G. Direct view of stress distribution in solid by mechanoluminescence. Applied Physics Letters. 1999;**74**:2414-2416

[2] Jha P, Khare A, Singh PK, Chandra VK, Sonwane VD. Ball impact induced elastico-mechanoluminescence for impact sensor. Journal of Luminescence. 2018;**195**:40-43

[3] Wang X, Xu C-N, Yamada H, Nishikubo K, Zheng X-G. Electro-mechano-optical conversions in Pr^{3+}-doped $BaTiO_3$–$CaTiO_3$ ceramics. Advanced Materials. 2005;**17**:1254-1258

[4] Feng A, Smet PF. A review of mechanoluminescence in inorganic solids: Compounds, mechanisms, models and applications. Materials. 2018;**11**:484

[5] Jeong SM, Song S, Joo K-I, Kim J, Hwang S-H, Jeong J, et al. Bright, wind-driven white mechanoluminescence from zinc sulphide microparticles embedded in a polydimethylsiloxane elastomer. Energy & Environmental Science. 2014;**7**:3338-3346

[6] Dengfeng P, Bing C, Feng W. Recent advances in doped mechanoluminescent phosphors. ChemPlusChem. 2015;**80**:1209-1215

[7] Wu C, Zeng S, Wang Z, Wang F, Zhou H, Zhang J, et al. Efficient mechanoluminescent elastomers for dual-responsive anticounterfeiting device and stretching/strain sensor with multimode sensibility. Advanced Functional Materials. 2018:1803168

[8] Olawale DO, Dickens T, Sullivan WG, Okoli OI, Sobanjo JO, Wang B. Progress in triboluminescence-based smart optical sensor system. Journal of Luminescence. 2011;**131**:1407-1418

[9] Zhang H, Yamada H, Terasaki N, Xu C-N. Blue light emission from stress-activated $CaYAl_3O_7$:Eu. Journal of the Electrochemical Society. 2008;**155**:J128-J131

[10] Zhang J-C, Zhao L-Z, Long Y-Z, Zhang H-D, Sun B, Han W-P, et al. Color Manipulation of intense multiluminescence from CaZnOS:Mn^{2+} by Mn^{2+} concentration effect. Chemistry of Materials. 2015;**27**:7481-7489

[11] Akiyama M, Xu C-N, Liu Y, Nonaka K, Watanabe T. Influence of Eu, Dy co-doped strontium aluminate composition on mechanoluminescence intensity. Journal of Luminescence. 2002;**97**:13-18

[12] Xie Y, Li Z. Triboluminescence: Recalling interest and new aspects. Chem. 2018;**4**:943-971

[13] Zink JI, Hardy GE, Sutton JE. Triboluminescence of sugars. The Journal of Physical Chemistry. 1976;**80**:248-249

[14] Chandra BP. Mechanoluminescence and piezoelectric behaviour of molecular crystals. Physica Status Solidi. 1981;**64**:395-405

[15] Chandra BP, Zink JI. Triboluminescence of triclinic crystals. Journal of Luminescence. 1981;**23**:363-372

[16] Hardy GE, Baldwin JC, Zink JI, Kaska WC, Liu P-H, Dubois L. Triboluminescence spectroscopy of aromatic compounds. Journal of the American Chemical Society. 1977;**99**:3552-3558

[17] Sweeting LM, Rheingold AL. Crystal structure and triboluminescence. 1. 9-Anthryl carbinols. The Journal of Physical Chemistry. 1988;**92**:5648-5655

[18] Wang C, Xu B, Li M, Chi Z, Xie Y, Li Q, et al. A stable tetraphenylethene derivative: Aggregation-induced emission, different crystalline polymorphs, and totally different mechanoluminescence properties. Materials Horizons. 2016;**3**:220-225

[19] Fontenot RS, Hollerman WA, Bhat KN, Aggarwal MD. Synthesis and characterization of highly triboluminescent doped europium tetrakis compounds. Journal of Luminescence. 2012;**132**:1812-1818

[20] Marchetti F, Di Nicola C, Pettinari R, Timokhin I, Pettinari C. Synthesis of a photoluminescent and triboluminescent copper(I) compound: An experiment for an advanced inorganic chemistry laboratory. Journal of Chemical Education. 2012;**89**:652-655

[21] Butler CT. Room-temperature deformation luminescence in alkali halides. Physical Review. 1966;**141**:750-757

[22] Rai RK, Upadhyay AK, Kher RS, Dhoble SJ. Mechanoluminescence, thermoluminescence and photoluminescence studies on Al_2O_3:Tb phosphors. Journal of Luminescence. 2012;**132**:210-214

[23] Akiyama M, Xu C-N, Nonaka K. Intense visible light emission from stress-activated ZrO_2:Ti. Applied Physics Letters. 2002;**81**:457-459

[24] Wang X, Zhang H, Yu R, Dong L, Peng D, Zhang A, et al. Dynamic pressure mapping of personalized handwriting by a flexible sensor matrix based on the mechanoluminescence process. Advanced Materials. 2015;**27**:2324-2331

[25] Li L, Wong K-L, Li P, Peng M. Mechanoluminescence properties of Mn^{2+}-doped BaZnOS phosphor. Journal of Materials Chemistry C. 2016;**4**:8166-8170

[26] Zhang H, Terasaki N, Yamada H, Xu C-N. Mechanoluminescence of europium-doped $SrAMgSi_2O_7$ (A=Ca, Sr, Ba). Japanese Journal of Applied Physics. 2009;**48**:04C109

[27] Sahu AK, Kore BP, Chowdhary PS, Nayar V, Dhoble SJ. Systematic study of photoluminescence, lyoluminescence and mechanoluminescence in Ce^{3+}- and Eu^{3+}-activated Li_3PO_4 phosphors. Luminescence. 2014;**29**:58-64

[28] Kamimura S, Yamada H, Xu C-N. Development of new elasticoluminescent material $SrMg_2(PO_4)_2$:Eu. Journal of Luminescence. 2012;**132**:526-530

[29] Mishra GC, Upadhyay AK, Dwiwedi SK, Dhoble SJ, Kher RS. Correlation between thermoluminescence and mechanoluminescence of γ-ray-irradiated Dy-doped BaB_4O_7 phosphors. Journal of Materials Science. 2012;**47**:2752-2756

[30] Zhang J-C, Long Y-Z, Wang X, Xu C-N. Controlling elastico-mechanoluminescence in diphase $(Ba,Ca)TiO_3$:Pr^{3+} by co-doping different rare earth ions. RSC Advances. 2014;**4**:40665-40675

[31] Zhang J-C, Long Y-Z, Yan X, Wang X, Wang F. Creating recoverable mechanoluminescence in piezoelectric calcium niobates through Pr^{3+} doping. Chemistry of Materials. 2016;**28**:4052-4057

[32] Dong T, Chao-Nan X, Akihito Y, Masayoshi F, Jou H, Xu-Guang Z. LiNbO3:Pr3+: A multipiezo material with simultaneous piezoelectricity and sensitive piezoluminescence. Advanced Materials. 2017;**29**:1606914

[33] Kamimura S, Yamada H, Xu C-N. Purple photochromism in Sr_2SnO_4:Eu^{3+} with layered perovskite-related structure. Applied Physics Letters. 2013;**102**:031110

[34] Upadhyay AK, Dhoble SJ, Kher RS. Mechanoluminescence properties of gamma-ray-irradiated $BaSO_4$:Eu phosphors. Luminescence. 2011;**26**:471-476

[35] Botterman J, KVd E, Baere ID, Poelman D, Smet PF. Mechanoluminescence in $BaSi_2O_2N_2$:Eu. Acta Materialia. 2012;**60**:5494-5500

[36] Moon JS, Seongkyu S, Soo-Keun L, Young HN. Color manipulation of mechanoluminescence from stress-activated composite films. Advanced Materials. 2013;**25**:6194-6200

[37] Shohag MAS, Tran SA, Ndebele T, Adhikari N, Okoli OI. Designing and implementation of triboluminescent materials for real-time load monitoring. Materials and Design. 2018;**153**:86-93

[38] Jeong SM, Song S, Lee S-K, Choi B. Mechanically driven light-generator with high durability. Applied Physics Letters. 2013;**102**:051110

[39] Sohn K-S, Park WB, Timilsina S, Kim JS. Mechanoluminescence of $SrAl_2O_4$:Eu^{2+}, Dy^{3+} under cyclic loading. Optics Letters. 2014;**39**:1410-1413

[40] Fan X-H, Zhang J-C, Zhang M, Pan C, Yan X, Han W-P, et al. Piezoluminescence from ferroelectric $Ca_3Ti_2O_7$:Pr^{3+} long-persistent phosphor. Optics Express. 2017;**25**:14238-14246

[41] Sohn K-S, Cho MY, Kim M, Kim JS. A smart load-sensing system using standardized mechano-luminescence measurement. Optics Express. 2015;**23**:6073-6082

[42] Smith CJ, Griffin SR, Eakins GS, Deng F, White JK, Thirunahari S, et al. Triboluminescence from pharmaceutical formulations. Analytical Chemistry. 2018;**90**:6893-6898

[43] Zhang J-C, Xu C-N, Kamimura S, Terasawa Y, Yamada H, Wang X. An intense elastico-mechanoluminescence material CaZnOS:Mn^{2+} for sensing and imaging multiple mechanical stresses. Optics Express. 2013;**21**:12976-12986

[44] Mao Q, Chen Z, Ji Z, Xi J. UV-assisted mechanoluminescence properties of $SrAl_2O_4$: (Eu,Dy) for impact sensing. Journal of Materials Science. 2017;**52**:8370-8376

[45] Xin Q, Zheren C, Meng S, Fengyu L, Wei F, Yudong L, et al. Printable skin-driven mechanoluminescence devices via nanodoped matrix modification. Advanced Materials. 2018;**30**:1800291

[46] Krishnan S, Van der Walt H, Venkatesh V, Sundaresan VB. Dynamic characterization of elastico-mechanoluminescence towards structural health monitoring. Journal of Intelligent Material Systems and Structures. 2017;**28**:2458-2464

[47] Suman T, Ho LK, Nam KY, Sik KJ. Optical evaluation of in situ crack propagation by using mechanoluminescence of $SrAl_2O_4$:Eu^{2+}, Dy^{3+}. Journal of the American Ceramic Society. 2015;**98**:2197-2204

[48] Scheiner M, Hammel E, Okoli OI. Ultraviolet priming of triboluminescence. Journal of Luminescence. 2018;**194**:803-805

[49] Xu C-N, Zheng X-G, Akiyama M, Nonaka K, Watanabe T. Dynamic visualization of stress distribution by mechanoluminescence image. Applied Physics Letters. 2000;**76**:179-181

[50] Terasaki N, Xu CN. Historical-log recording system for crack opening and growth based on mechanoluminescent flexible sensor. IEEE Sensors Journal. 2013;**13**:3999-4004

[51] Kim JS, Kwon Y-N, Sohn K-S. Dynamic visualization of crack

propagation and bridging stress using the mechano-luminescence of $SrAl_2O_4$: (Eu,Dy,Nd). Acta Materialia. 2003;**51**:6437-6442

[52] Yoshida A, Liu L, Tu D, Kainuma S, Xu C-N. Mechanoluminescent testing as an efficient inspection technique for the management of infrastructures. Journal of Disaster Research. 2017;**12**:506-514

[53] Fujio Y, Xu C-N, Terasawa Y, Sakata Y, Yamabe J, Ueno N, et al. Sheet sensor using $SrAl_2O_4$:Eu mechanoluminescent material for visualizing inner crack of high-pressure hydrogen vessel. International Journal of Hydrogen Energy. 2016;**41**:1333-1340

[54] Yang Y, Zheng S, Fu X, Zhang H. Remote and portable mechanoluminescence sensing system based on a $SrAl_2O_4$:Eu,Dy film and its potential application to monitoring the safety of gas pipelines. Optik. 2018;**158**:602-609

[55] Shohag MAS, Jiang Z, Hammel EC, Braga Carani L, Olawale DO, Dickens TJ, et al. Development of friction-induced triboluminescent sensor for load monitoring. Journal of Intelligent Material Systems and Structures. 2018;**29**:883-895

[56] Zhang J, Bao L, Lou H, Deng J, Chen A, Hu Y, et al. Flexible and stretchable mechanoluminescent fiber and fabric. Journal of Materials Chemistry C. 2017;**5**:8027-8032

[57] Wong M-C, Chen L, Tsang M-K, Zhang Y, Hao J. Magnetic-induced luminescence from flexible composite laminates by coupling magnetic field to piezophotonic effect. Advanced Materials. 2015;**27**:4488-4495

[58] Terasaki N, Yamada H, Xu C-N. Ultrasonic wave induced mechanoluminescence and its application for photocatalysis as ubiquitous light source. Catalysis Today. 2013;**201**:203-208

[59] Moon JS, Seongkyu S, Hyunmin K, Kyung-Il J, Hideo T. Mechanoluminescence color conversion by spontaneous fluorescent-dye-diffusion in elastomeric zinc sulfide composite. Advanced Functional Materials. 2016;**26**:4848-4858

[60] Wong M-C, Chen L, Bai G, Huang L-B, Hao J. Temporal and remote tuning of piezophotonic-effect-induced luminescence and color gamut via modulating magnetic field. Advanced Materials. 2017;**29**:1701945

[61] Jeong SM, Song S, Kim H. Simultaneous dual-channel blue/green emission from electro-mechanically powered elastomeric zinc sulphide composite. Nano Energy. 2016;**21**:154-161

[62] Wang X, Que M, Chen M, Han X, Li X, Pan C, et al. Full dynamic-range pressure sensor matrix based on optical and electrical dual-mode sensing. Advanced Materials. 2017;**29**:1605817

[63] Zhang H, Peng D, Wang W, Dong L, Pan C. Mechanically induced light emission and infrared-laser-induced upconversion in the Er-doped CaZnOS multifunctional piezoelectric semiconductor for optical pressure and temperature sensing. The Journal of Physical Chemistry C. 2015;**119**:28136-28142

[64] Gun Jin Y, Mohammad Reza R, Amir Hossein G, Gong-Cheol L, Jun-Seong C. Stress sensing performance using mechanoluminescence of $SrAl_2O_4$:Eu (SAOE) and $SrAl_2O_4$:Eu, Dy (SAOED) under mechanical loadings. Smart Materials and Structures. 2013;**22**:055006

[65] Someya S, Ishii K, Munakata T, Saeki M. Lifetime-based measurement of stress during

cyclic elastic deformation using mechanoluminescence of $SrAl_2O_4:Eu^{2+}$. Optics Express. 2014;**22**:21991-21998

[66] Ali Imani A, Mohammad Reza R, Gun Jin Y. Quantitative full-field strain measurements by SAOED ($SrAl_2O_4:Eu^{2+}$, Dy^{3+}) mechanoluminescent materials. Smart Materials and Structures. 2016;**25**:095032

[67] Terasaki N, Xu C-N, Imai Y, Yamada H. Photocell system driven by mechanoluminescence. Japanese Journal of Applied Physics. 2007;**46**:2385

[68] Huajing F, Xiandi W, Qiang L, Dengfeng P, Qingfeng Y, Caofeng P. A stretchable nanogenerator with electric/light dual-mode energy conversion. Advanced Energy Materials. 2016;**6**:1600829

[69] Terasaki N, Zhang H, Imai Y, Yamada H, Xu C-N. Hybrid material consisting of mechanoluminescent material and TiO_2 photocatalyst. Thin Solid Films. 2009;**518**:473-476

[70] Hyodo K, Xu C, Mishima H, Miyakawa S. Optical Stress Imaging for Orthopedic Biomechanics-Comparison of Thermoelastic Stress Analysis and Developed Mechanoluminescent Method. Berlin, Heidelberg: Springer Berlin Heidelberg; 2010. pp. 545-548

[71] Jiang Y, Wang F, Zhou H, Fan Z, Wu C, Zhang J, et al. Optimization of strontium aluminate-based mechanoluminescence materials for occlusal examination of artificial tooth. Materials Science and Engineering: C. 2018;**92**:374-380